Metrol. Meas. Syst., Vol. 32 (2025) No. 1, pp. 1–14
DOI: 10.24425/mms.2025.152773

PAN POLSKA AKADEMIA NAUK

METROLOGY AND MEASUREMENT SYSTEMS
Index 330930, ISSN 0860-8229
www.metrology.wat.edu.pl

M&MS

KERNEL EXTREME LEARNING MACHINE COMBINED WITH GRAY WOLF OPTIMIZATION FOR TEMPERATURE COMPENSATION IN PRESSURE SENSORS

Huan Wang, Ting Wu, Pan Liu, Yijun Zou, Qinghua Zeng

School of Aeronautics and Astronautics, Sun Yat-sen University, Shenzhen, China, (✉ *wangh658@mail2.sysu.edu.cn*)

Abstract

In order to improve the measurement accuracy of pressure sensors, a method based on gray wolf optimization (GWO) to optimize kernel extreme learning machine (KELM) is proposed to address the problem of nonlinear drift that can be easily affected by temperature in the working environment. Firstly, the fast search capability of the GWO algorithm is used to find optimal regularization coefficients and kernel function parameters of the KELM algorithm; secondly, the random mapping of the traditional ELM algorithm is replaced by the kernel mapping of the KELM algorithm to improve the generalization and stability degradation brought by the random assignments. Finally, the voltage signal values under different temperature and pressure environments are obtained through calibration experiments and compensated by the GWO-KELM algorithm. The results show that the GWO-KELM method has a better compensation effect compared with the traditional BP neural network with a full-scale error of 0.13% (FS), the ELM algorithm with a full-scale error of 0.12%FS, and the KELM algorithm with a full-scale error of 0.12% in the range of 0 to 700 kPa absolute pressure and –40° to 70°. The full-scale error is only 0.07% and the maximum absolute error is as low as 0.5446 kPa, which improves the accuracy index by one order of magnitude.

Keywords: Gray wolf optimization, kernel extreme learning machine, pressure sensor, temperature compensation.

1. Introduction

Silicon piezoresistive pressure sensors are widely used in cutting-edge applications such as medical devices [1–3], robotics [4], industrial automation [5], military defense [6], and aerospace [7,8],. Despite this, pressure sensors face many challenges from a variety of applications and operating conditions. A precision measurement requires a pressure sensor with a high accuracy (less than 0.1% FS) [9] and stable performance over a wide temperature range (*e.g.*, -40 to 70°C). The accuracy of the pressure sensor is therefore a key factor in determining its performance indicators in engineering [10]. There is, however, a high degree of sensitivity to temperature and nonlinear drift in pressure sensor accuracy metrics, which seems inevitable [11]. In the case of the common piezoresistive pressure sensor, the operating conditions of its internal resistance will also change when the ambient temperature changes, affecting the sensor's output. For this reason, compensating the pressure sensor must be done in order to eliminate interference caused by temperature changes [12,13].

Article history: received June 26, 2024; revised September 25, 2024; accepted October 3, 2024; available online November 18, 2024.

Temperature compensation can be achieved in two ways: through hardware compensation and through software compensation. There are several methods for hardware compensation available, including strain gauge self-compensation [14], compensation for bridge circuits [15], compensation for auxiliary measurements [16], and compensation for thermistor types [17]. To a certain extent, these compensation methods can achieve temperature compensation. However, integration and miniaturization difficulties prevent intelligent sensor development [18, 19]. Among the software compensation methods there are the interpolation fitting method [20], regression analysis method [21], neural network method [22, 23], *etc.* As compared to hardware compensation, software algorithmic compensation is more robust and requires fewer manufacturing processes.

Currently, most pressure sensor temperature compensation research relies mostly on software. These methods produce good compensation results when combining neural networks with optimization algorithms. To address the problem of low pressure scanner accuracy due to temperature variations during measurement, Wang *et al.* [24] proposed a *backward propagation* (BP) neural network based on the *whale optimization algorithm* (WOA). Ge *et al.* [25] compensated for temperature drift in fiber optic F-P pressure sensors using a wavelet neural network based on a genetic algorithm. Xie *et al.* [26] proposed an improved algorithm for optimizing *radial basis function* (RBF) neural networks for pressure sensors to achieve pressure compensation by using *Dynamic Quantum Particle Swarm Optimization* (DQPSO).

As a result, neural networks such as BP and RBF suffer from the problems of slow operation speed, poor generalization ability, and insufficient compensation effect when improving accuracy, which becomes their main bottleneck. Therefore, a new structure with fast learning speed, easy to obtain the global optimal solution, and strong generalization capability has become the focus and hot area of current research. Data mining and time series forecasting have gradually gained popularity in recent years using prediction methods based on the *Extreme Learning Machine* (ELM) [27, 28]. This single hidden layer neural network is significantly faster, more algorithmically sound, and more generalizable than traditional neural networks. However, the incorporation of kernel functions into *Kernel Extreme Learning Machine* (KELM) algorithms can often achieve better generalization performance than traditional ELM algorithms for nonlinear feature learning [29, 30]. In addition, it helps solve data modeling and prediction tasks involving complex nonlinear relationships [31]. Zou *et al.* used Aquila Optimizer to optimize the hybrid polynomial KELM to generate more data for sensor compensation, resulting in 0.03% FS in the range of –250 to +250 kPa [32]. Li *et al.* used the coupled simulated annealing algorithm and the simplex algorithm combined with KELM to achieve the desired synthetic compensation performance at pressures from -1000 kPa to 1000 kPa and temperatures from –20°C to 70°C [33]. All of the above methods show that KELM has a great potential for temperature compensation in pressure sensors, but a combination of different optimization algorithms is needed to produce better compensation when specific to the characteristics of different types of sensors.

Therefore, in this paper, a *Gray Wolf Optimization* (GWO) algorithm is proposed to optimize KELM's temperature compensation strategy, which is applied to silicon piezoresistive pressure sensors. By using this strategy, KELM updates will be faster and more flexible. KELM not only takes advantage of the fast iteration of the GWO to find the optimal solution, but also achieves high prediction accuracy and compensation stability thanks to the fast iteration of the algorithm. A BP and ELM model is first used for analysis; a KELM model is then developed by adding a kernel function; finally, a hybrid algorithm named GWO-KELM is developed using the GWO model. To verify the validity of the proposed model, we will compare the performance errors of the BP model, ELM model, and KELM model. Moreover, to enhance the practicality of the algorithm, we will conduct compensation experiments using real pressure sensor calibration data. By using examples, it can be demonstrated that the method can indeed enhance sensor accuracy to a high level.

The sections of the article are described as follows: Section 2 discusses the fundamentals of sensor compensation, introduces Gray Wolf Optimization and the Kernel Extreme Learning Machine, and proposes a hybrid GWO-KELM compensation algorithm. In Section 3, we describe a method for obtaining experimental data for calibrating pressure sensors as well as the experimental schematic and the actual data gathered. Section 4 compares the compensation results of the GWO-KELM model with various compensation methods to verify the feasibility and effectiveness of temperature compensation in pressure sensors. Section 5 concludes this study.

2. Methods for temperature compensation in pressure sensors

2.1. Pressure sensor temperature compensation principle

As shown in Fig. 1 below, a schematic diagram of a pressure sensor using the GWO algorithm to optimize the KELM for temperature compensation is demonstrated. A pressure sensor core and a temperature sensor measure external pressure and ambient temperature, respectively. The output signal of the pressure sensor and temperature signal of the temperature sensor are both fed into the KELM's input layer.

An optimal regularization coefficient and kernel function parameter are found using the GWO in this system. This optimizes the performance of the KELM. As the final temperature compensation operation is performed using the KELM, it is used to predict the pressure value first. To determine the difference, it compares the predicted value with the measured value. A GWO algorithm is then used to continuously optimize the parameters of the KELM in order to minimize the difference, thus completing the temperature compensation process. It is a repeated process in which the parameters of the KELM are constantly adjusted in order to gradually achieve the optimal state, which allows the output of the pressure sensor to be compensated for temperature changes and the system to be more accurate and stable.

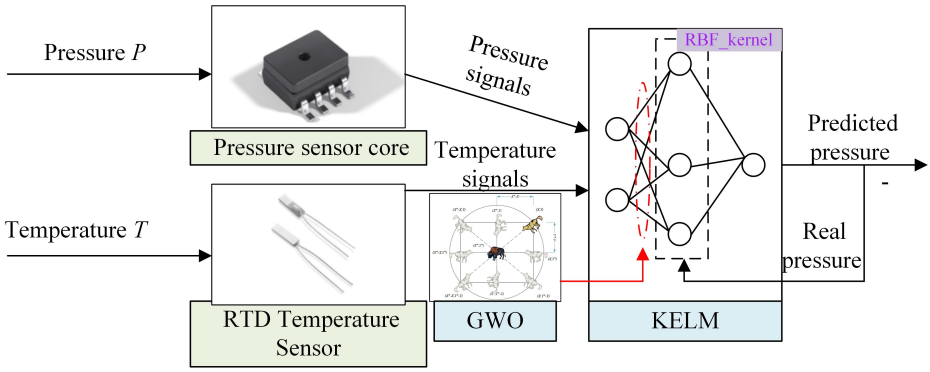

Fig. 1. Temperature compensation schematic diagram.

2.2. GWO-KELM

2.2.1. KELM

KELM (*Kernel Extreme Learning Machine*) employs a simple single hidden layer structure [34]. It completes the learning process by randomly selecting regularization coefficients and kernel parameters to compute output weights. Compared with traditional gradient algorithms, KELM

avoids problems such as local minima and overfitting, and has excellent learning and generalization capabilities [35, 36]. KELM is an efficient and easy-to-implement model. Its ELM network structure practically used in this paper is shown in Fig. 2.

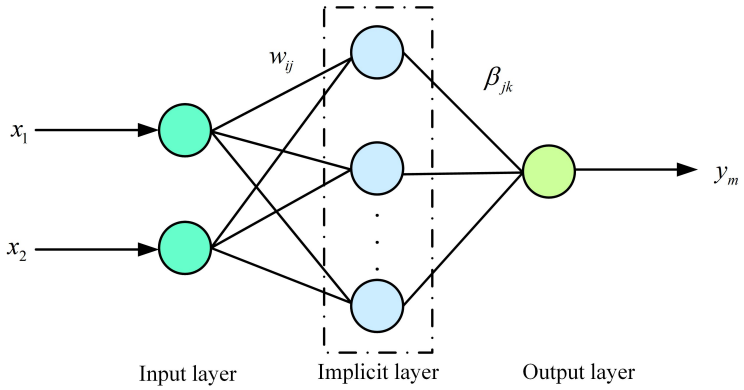

Fig. 2. Extreme learning machine network structure.

2.2.2. GWO

Gray Wolf Optimization (GWO) is a novel heuristic algorithm inspired by gray wolves' intrinsic system and hunting behavior [38]. Its goal is to find the optimal solution by simulating gray wolf hunting patterns. In the natural environment, gray wolves are top predators in the food chain, exhibiting strong group collaboration and hunting strategies. Gray wolf groups maintain a strict social structure and hierarchy within the group [39]. This forms a clear hierarchy of leadership and division of labor, as shown in Fig. 3.

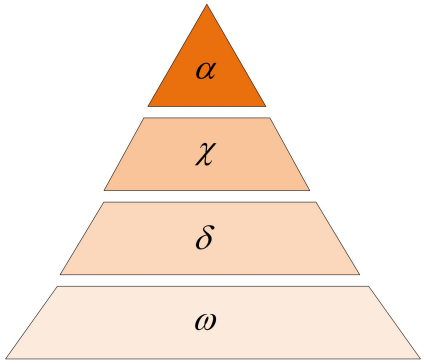

Fig. 3. Hierarchy diagram for the Gray Wolf Optimization.

The gray wolf algorithm divides wolves into four types. The first type is the α wolf, which is in the leadership position of the pack. The second type is the β wolf, which strictly follows the α wolf leadership and passes information and mediates disputes within the pack. In the absence of the α, the β wolves control all other wolves. Lastly, the δ wolves lead only the ω wolves within the pack and perform basic tasks. Finally, the fourth category are the ω wolves, which are located at the bottom of the pack hierarchy and obey higher-ranking wolves' orders. Fig. 4. shows a schematic of the search process for optimal solutions.

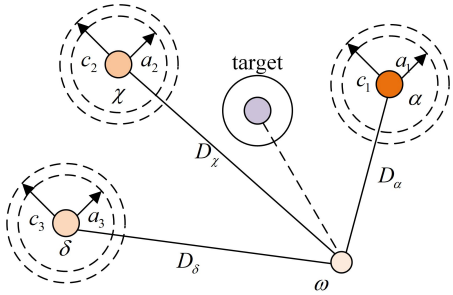

Fig. 4. Explanatory chart for gray wolf seeking superiority.

The separation distance D between the gray wolf and the target can be expressed as follows in the surrounding behavior of the gray wolf algorithm:

$$D = |(r) - (r)|, \tag{1}$$

where r is the number of iterations; is the position of the target. $\overrightarrow{X'}$ denotes the position of the gray wolf.

In order to dynamically adjust the position, the wolves need to perform a positional update of the distance, which allows the wolves to approach the target from different vantage points, with the update equation being

$$\overrightarrow{X'}(r+1) = \overrightarrow{X'_p}(r) - \overrightarrow{A}\overrightarrow{D}, \tag{2}$$

$$\overrightarrow{A} = 2\overrightarrow{\alpha}\overrightarrow{r_1} - \overrightarrow{\alpha}, \tag{3}$$

$$\overrightarrow{C} = 2\overrightarrow{r_2}, \tag{4}$$

where is the convergence factor; , are belong to $[0, 1]$; and are the coefficient vectors.

Once the pack has successfully surrounded the target, search behavior begins. α, β, and δ wolves are positioned closest to the target. Its search behavior can be expressed as

$$D_\alpha = \overrightarrow{C_1}\overrightarrow{X'_\alpha}(r) - \overrightarrow{X'}(r) \tag{5}$$

$$D_\chi = \overrightarrow{C_2}\overrightarrow{X'_\chi}(r) - \overrightarrow{X'}(r) \tag{6}$$

$$D_\delta = \overrightarrow{C_3}\overrightarrow{X'_\delta}(r) - \overrightarrow{X'}(r) \tag{7}$$

$$\overrightarrow{X'_1}(r+1) = \overrightarrow{X'_\alpha}(r) - \overrightarrow{A_1}\overrightarrow{D_\alpha} \tag{8}$$

$$\overrightarrow{X'_2}(r+1) = \overrightarrow{X'_\chi}(r) - \overrightarrow{A_2}\overrightarrow{D_\chi} \tag{9}$$

$$\overrightarrow{X'_3}(r+1) = \overrightarrow{X'_\delta}(r) - \overrightarrow{A_3}\overrightarrow{D_\delta} \tag{10}$$

$$\overrightarrow{X'}(r+1) = \frac{1}{3}\left[\overrightarrow{X'_1}(r+1) + \overrightarrow{X'_2}(r+1) + \overrightarrow{X'_3}(r+1)\right] \tag{11}$$

2.2.3. GWO-KELM algorithm design

In addition to the regularization coefficients, the kernel function parameters also directly affect the prediction efficiency and accuracy of the KELM algorithm. On the one hand, inappropriate selection may cause the algorithm to arrive at a poor solution, which affects the accuracy of

compensation [40]. On the other hand, it requires multiple trainings to find the most suitable regularization coefficients and kernel function parameters, which is a process of randomness and chance and impacts the actual effect of the KELM [41].

In this study, the excellent search capability of the GWO is utilized to iteratively search for the optimal regularization coefficients and kernel function parameters of the KELM, which can use the advantages of the kernel limit learning machine. The steps to temperature compensation of the KELM based on the GWO are as follows:

1. Each of the obtained pressure sensor and temperature sensor datasets (corresponding to the inputs of the KELM network, respectively) are divided into a training set and a test set (7:3) and normalized.
2. Initialize the gray wolf algorithm parameters. Calculate the current gray wolf population status.
3. Calculate the current population fitness value and update the coefficient vector $\overrightarrow{A'}$ and $\overrightarrow{C'}$.
4. Calculate the distance and update the position, and search for optimization.
5. Calculate whether the fitness is optimal. If it is reached, calculate the optimal gray wolf position, *i.e.*, the regularization coefficient and kernel function parameter of the KELM; if it is not determined, check iterations. If not, adjust the coefficient vector sum and iterate the training again.
6. Relate the optimal regularization coefficients and kernel functions to the KELM for algorithm training.
7. Output the most accurate predicted pressure value.

3. Temperature calibration experiment

3.1. Experimental system

The experimental system for collecting measurement data from a silicon piezoresistive gas pressure sensor is shown in Fig. 5. The main apparatus of this experimental system is composed of a constant temperature test chamber, a pressure calibrator, a gas pressure sensor, and a test computer. First, the pressure sensor is connected to the pressure calibrator through a gas hose. The pressure calibrator will provide a variable pressure environment for the sensor. Next, the

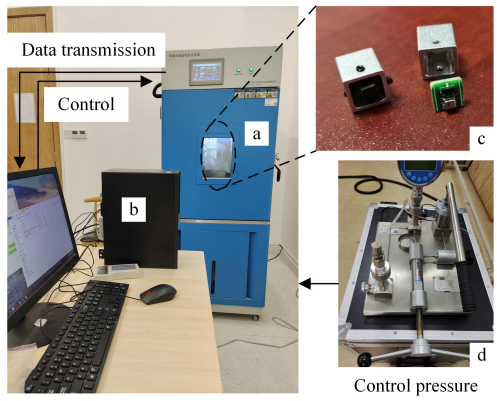

Fig. 5. Pressure sensor experiment acquisition system diagram (a) test chamber; (b) test computer; (c) gas pressure sensor; (d) pressure calibrator.

connected pressure transducer is placed in a thermostatic test chamber. The thermostat simulates different ambient temperatures for the sensor. Finally, the signals sensed by the transducer from the ambient environment are transmitted via a data cable to the test computer for display.

3.2. Data acquisition

In order to analyze and record the characteristics of sensors with temperature changes, in the experiment the nominal absolute pressure range from 0 to 700 kPa pressure sensor core was selected as a test. At the same time, a *resistance temperature detecto*r (RTD) sensor monitored the current ambient temperature in a temperature chamber together with the pressure sensor core.

In order to achieve 5°C intervals, 23 temperature points ranging from –40°C to 70°C were selected for this experiment. The experiment was conducted by sequentially applying pressures from 0 to 700 kPa, 70 kPa at a time, for a total of 11 pressure values. At each time when the specified temperature point was reached, the operation of holding the temperature for 2 hours was performed. The power was turned on for 10 minutes to start the pressure recording.

4. Compensation results and analysis

4.1. Parameterization and evaluation indicators

In order to investigate the performance of this paper's algorithm for compensating pressure sensors in different temperature environments, MATLAB 2020a is used for temperature compensation experiments.

According to the temperature compensation step assumed in Section 2.2.3, the population number of the GWO is set to 40 and the maximum number of iterations to 10. For the KELM, the input layer neurons is set to 2 and the output layer neurons to 1. In the compensation process of the GWO for optimizing the KELM, the fitness function selected the value of the error computed each time. When the error is smaller, the corresponding compensation accuracy value is higher. The *full-scale error* (FS) [42] of the sensor and the *mean absolute error* (MAE), *root mean square error* (RMSE), and *mean absolute percentage error* (MAPE), which are commonly used for prediction, are selected to evaluate the algorithm's compensation performance [43, 44].

The specific formula for its error evaluation index is:

$$e_{\mathrm{FS}} = \frac{1}{P_{\mathrm{FS}}} \max |y_i - \hat{y}_i|, \tag{12}$$

$$e_{\mathrm{MAE}} = \frac{1}{N'} \sum_{i=1}^{N'} |y_i - \hat{y}_i|, \tag{13}$$

$$e_{\mathrm{RMSE}} = \sqrt{\frac{1}{N'} \sum_{i=1}^{N'} (y_i - \hat{y}_i)^2}, \tag{14}$$

$$e_{\mathrm{MAPE}} = \frac{1}{N'} \sum_{i=1}^{N'} \frac{|y_i - \hat{y}_i|}{y_i} \times 100\text{‰}, \tag{15}$$

where P_{FS} is the full-scale pressure; N' is the number of samples; y_i is the standard pressure value at each actual temperature; and $\hat{y}_i$ is the compensated pressure value.

4.2. Compensation results and error analysis

After setting the parameters, the algorithm program is run and the fitness curve of the GWO for optimization is obtained. It is shown in Fig. 6.

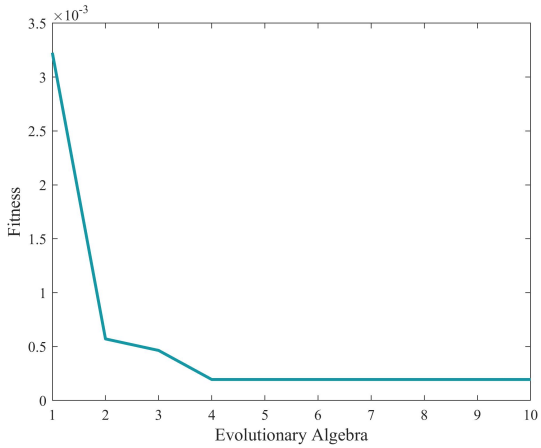

Fig. 6. Graph of the fitness function.

Figure 6 demonstrates that the gray wolf algorithm quickly searches for optimality during preliminary iterations. After four to five iterations, the optimal fitness value is immediately found (The final result time to iterate out the pressure value is 0.34 s.). The gray wolf position at this time is the optimal regularization coefficient and kernel function parameters of the KELM algorithm. Through the compensation of the KELM model, the comparison between the high-precision pressure value predicted by the algorithm and the actual real pressure value was finally obtained as shown in Fig. 7(a), and the absolute error distribution of the test set after compensation is shown in Fig. 7(b).

In order to see the comparison effect more clearly, the following figure is shown. Fig. 7(a) shows the pressure value after GWO-KELM compensation compared with the real value between 200–600 samples in the test set and the pressure range of 500–600 kPa. It can be seen that the

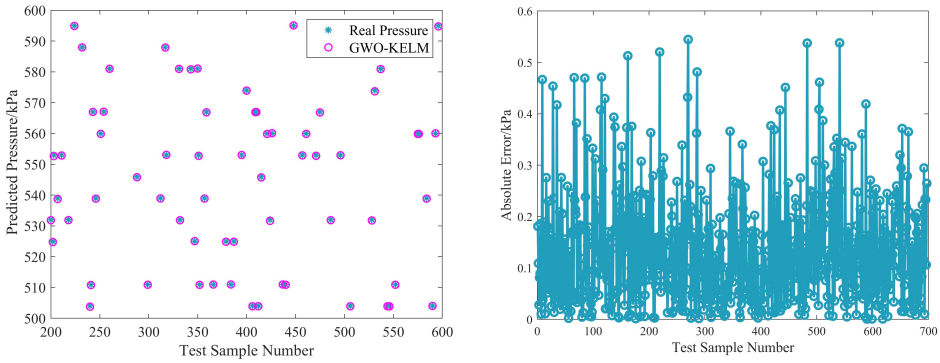

(a) (b)

Fig. 7. (a) GWO-KELM compensated value vs. true value; (b) Absolute error distribution plot.

compensated values overlap with the true values with excellent consistency, *i.e.*, high accuracy after compensation. Figure 7(b) shows that the maximum absolute error after compensation by the GWO-KELM algorithm is only 0.5446 kPa, and its corresponding full-scale error is 0.0778% FS.

At the same time, to compare the compensation effect of the GWO-KELM algorithm more clearly, the design ELM, BP neural network, and KELM algorithms are tested together. The relative error distribution is obtained as shown in Fig. 8. It can be seen that the relative errors of the BP neural network and KELM algorithms are larger. These errors are 0.05509 and 0.05661, respectively. The effect of the KELM optimized by the GWO is obviously improved, and its maximum relative error is reduced to 0.02036, which further exerts the advantages of the KELM, and also improves the smoothness of its compensation, which greatly avoids being affected by the regularization coefficients and kernel function parameters.

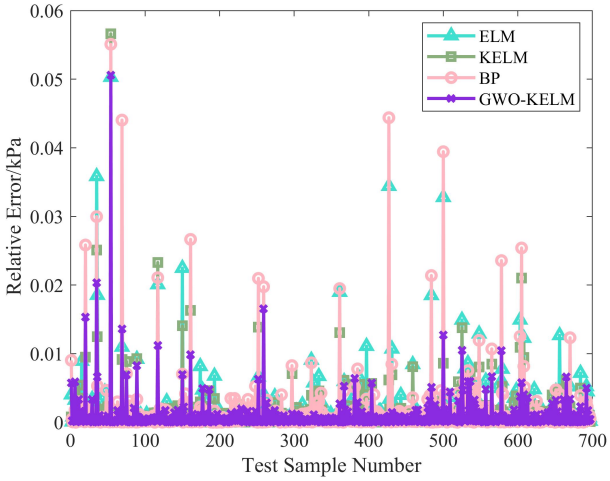

Fig. 8. Relative error distribution for different algorithms.

Based on the above test results, the error metrics of different algorithms are plotted as shown in Fig. 9. From the figure, it can be clearly seen that the MAE, RMSE, and MAPE error metrics of the GWO-KELM algorithm are at the lowest values among several algorithms. Therefore, the algorithm is superior in dealing with the temperature compensation problems. In addition to this, both the BP and ELM algorithms are at a higher level in terms of error metrics, indicating that the two algorithms have room for further improvement in dealing with the compensation problem.

So far, we have given the key indicators of the maximum absolute error and full-scale error as shown in Table 1:

Table 1. Comparison of key accuracy indicators for pressure

Model	Maximum absolute error (kPa)	FS (%)
BP	0.9099	0.1300
ELM	0.8601	0.1229
KELM	0.8492	0.1213
GWO-KELM	0.5446	0.0778

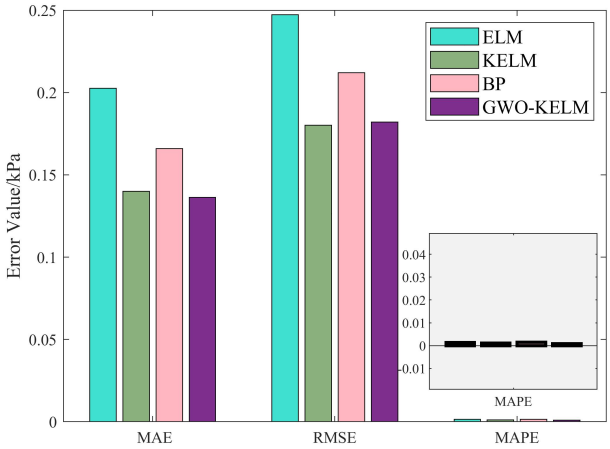

Fig. 9. Comparison of error metrics of different algorithms.

In the key indexes of the pressure sensors given in Table 1, it can be seen that the accuracy of the pressure sensors compensated by GWO-KELM is improved from the order of 1 part in a thousand to the order of 7 parts in 10,000 in comparison with the remaining three algorithms, which strongly indicates the effectiveness of the algorithms presented in this paper.

5. Conclusion

In this paper, we propose the use of GWO-KELM model to deal with the temperature compensation in gas pressure sensors to illustrate the effectiveness and reliability of the method. The main conclusions are as follows:

1. An innovative GWO-KELM gas pressure sensor compensation algorithm is proposed. The KELM algorithm improves solution accuracy. This is done by improving the ELM algorithm's poor handling of nonlinear problems, and then using the Gray Wolf Optimization Algorithm strategy.
2. For the experimentally collected data, the GWO-KELM algorithm converges to the target values quickly, showing strong optimization seeking ability.
3. From the experimental results, it can be seen that the GWO-KELM method has a better compensation effect. It achieves an accuracy of 0.07%FS in the full temperature range of the adiabatic pressure sensor 0-700 kPa, which is higher than the ELM and KELM accuracy of 0.12%FS. Compared to BP neural networks, it is an order of magnitude higher. Pressure sensors can be improved in accuracy and training time with this technology.

The GWO-KELM model can provide guidance for temperature compensation in gas pressure sensors. However, the model has some limitations. We will work on developing different models with higher compensation accuracy for different compensation types of silicon piezoresistive pressure sensors.

Acknowledgements

This work was supported by the National Natural Science Foundation of China (No. 61174120) and the Scientific Research and Innovation Program of the Chinese Academy of Management Sciences (No. JKSC14568).

References

[1] Xu, T., Wang, H., Xia, Y., Zhao, Z., Huang, M., Wang, J., Zhao, L., Zhao, Y., & Jiang, Z. (2017). Piezoresistive pressure sensor with high sensitivity for medical application using peninsula-island structure. *Frontiers of Mechanical Engineering*, *12*(4), 546–553. https://doi.org/10.1007/s11465-017-0447-9

[2] Pramanik, C., & Saha, H. (2006). Low Pressure Piezoresistive Sensors for Medical Electronics Applications. *Materials and Manufacturing Processes*, *21*(3), 233–238. https://doi.org/10.1080/10426910500464446

[3] Ginggen, A., Tardy, Y., Crivelli, R., Bork, T., & Renaud, P. (2008). A Telemetric Pressure Sensor System for Biomedical Applications. *IEEE Transactions on Biomedical Engineering*, *55*(4), 1374–1381. https://doi.org/10.1109/tbme.2007.913908

[4] Gao, Y., Xiao, T., Li, Q., Chen, Y., Qiu, X., Liu, J., Bian, Y., & Xuan, F. (2022). Flexible microstructured pressure sensors: design, fabrication and applications. *Nanotechnology*, *33*(32), 322002. https://doi.org/10.1088/1361-6528/ac6812

[5] Jakoby, B., Eisenschmid, H., & Herrmann, F. (2002). The potential of microacoustic SAW- and BAW-based sensors for automotive applications - a review. *IEEE Sensors Journal*, *2*(5), 443–452. https://doi.org/10.1109/jsen.2002.806748

[6] Han, X., Du, W., Chen, M., Wang, X., Zhang, X., Li, X., Li, J., Peng, Z., Pan, C., & Wang, Z.L. (2017). Visualization Recording and Storage of Pressure Distribution through a Smart Matrix Based on the Piezotronic Effect. *Advanced Materials*, *29*(26). https://doi.org/10.1002/adma.201701253

[7] Javed, Y., Mansoor, M., & Shah, I.A. (2019). A review of principles of MEMS pressure sensing with its aerospace applications. *Sensor Review*, *39*(5), 652–664. https://doi.org/10.1108/sr-06-2018-0135

[8] Angelidis, D.T. (1992). Optical micromachined pressure sensor for aerospace applications. *Optical Engineering*, *31*(8), 1638. https://doi.org/10.1117/12.58838

[9] Cheng, C., Yao, J., Xue, H., Lu, Y., Wang, J., Chen, D., & Chen, J. (2022). A MEMS Resonant Differential Pressure Sensor with High Accuracy by Integrated Temperature Sensor and Static Pressure Sensor. *IEEE Electron Device Letters*, *43*(12), 2157–2160. https://doi.org/10.1109/led.2022.3211886

[10] Zhao, C., & Kong, D. (2020). An indirect comparison quasi-static calibration method for piezoelectric pressure sensors based on an inverse model. *Measurement*, *159*, 107778. https://doi.org/10.1016/j.measurement.2020.107778

[11] Yue, Y.-L., Xu, S.-J., & Zuo, X. (2022). Nonlinear correction method of pressure sensor based on data fusion. *Measurement*, *199*, 111303. https://doi.org/10.1016/j.measurement.2022.111303

[12] Tang, Z., Wu, W., Gao, J., Yang, P., Hussain, A., Luo, J., Tao, R., Fu, C., & Li, T. (2022). Improving Water Pressure Measurement Using Temperature-Compensated Wireless Passive SAW Bidirectional RDL Pressure Sensor. *IEEE Transactions on Instrumentation and Measurement*, *71*, 1–11. https://doi.org/10.1109/tim.2021.3120146

[13] Pereira, R. dos S., & Cima, C.A. (2021). Thermal Compensation Method for Piezoresistive Pressure Transducer. *IEEE Transactions on Instrumentation and Measurement*, *70*, 1–7. https://doi.org/10.1109/tim.2021.3092789

[14] Zhang, C.C., Kang, Z.P., Zhao, N., Lei, P. and Yan, B. (Mar 2023). A Bilayer Thin-Film Strain Gauge with Temperature Self-Compensation. *IEEE Sens. J.*, 23, 6, 5601–5608. https://doi.org/10.1109/jsen.2023.3238328

[15] Zhao, G., Yin, J., Wu, L., & Feng, Z. (2020). Ultrastable and Low-Noise Self-Compensation Method for Circuit Thermal Drift of Eddy Current Sensors Based on Analog Multiplier. *IEEE Transactions on Industrial Electronics*, *67*(10), 8851–8859. https://doi.org/10.1109/tie.2019.2949511

[16] Ameli, A., Ghafouri, M., Salama, M.M.A., & El-Saadany, E.F. (2022). An Auxiliary Framework to Mitigate Measurement Inaccuracies Caused by Capacitive Voltage Transformers. *IEEE Transactions on Instrumentation and Measurement*, *71*, 1–11. https://doi.org/10.1109/tim.2022.3142040

[17] Anandanatarajan, R., Mangalanathan, U., & Gandhi, U. (2022). Deep Neural Network Based Linearization and Cold Junction Compensation of Thermocouple. *IEEE Transactions on Instrumentation and Measurement*, 1–1. https://doi.org/10.1109/tim.2022.3227982

[18] Pan, Q., Sun, Y., Su, M., Chen, S., Cai, Z., Zhang, Z., Zou, M., Chen, B., Mikhailova, J.V., Zuev, D., & Song, Y. (2022). Circular Subwavelength Photodetectors for 3D Space Exploration. *Advanced Optical Materials*, *10*(6). https://doi.org/10.1002/adom.202102163

[19] Long, H., Zhang, L., Ma, H., Li, J., Xia, J., Zhang, Y., & Chen, J. (2022). Heterogeneous Integration System in Display (HISiD) for Next-Generation Terminal Device. *IEEE Transactions on Components, Packaging and Manufacturing Technology*, *12*(5), 731–739. https://doi.org/10.1109/tcpmt.2022.3167729

[20] Yang, J., Yan, T., & Sun, W. (2023). Polynomial Fitting and Interpolation Method in TDOA Estimation of Sensors Network. *IEEE Sensors Journal*, *23*(4), 3837–3847. https://doi.org/10.1109/jsen.2022.3232625

[21] Li, Y., Yao, S., Zhang, R., & Yang, C. (2020). Analyzing host security using D-S evidence theory and multisource information fusion. *International Journal of Intelligent Systems*, *36*(2), 1053–1068. https://doi.org/10.1002/int.22330

[22] Badawi, D., Agambayev, A., Ozev, S., & Cetin, A.E. (2021). Real-Time Low-Cost Drift Compensation for Chemical Sensors Using a Deep Neural Network with Hadamard Transform and Additive Layers. *IEEE Sensors Journal*, *21*(16), 17984–17994. https://doi.org/10.1109/jsen.2021.3084220

[23] Tsai, P.-C., Cheng, C.-C., Chen, W.-J., & Su, S.-J. (2020). Sensor placement methodology for spindle thermal compensation of machine tools. *The International Journal of Advanced Manufacturing Technology*, *106*(11–12), 5429–5440. https://doi.org/10.1007/s00170-020-04932-8

[24] Wang, H., Zeng, Q., Zhang, Z., & Zou, Y. (2023). A novel whale-based algorithm for optimizing the ANN approach: application to temperature compensation in pressure scanner calibration systems. *Measurement Science and Technology*, *34*(9), 095904. https://doi.org/10.1088/1361-6501/acd26d

[25] Ge, Y., Shen, L., & Sun, M. (2021). Temperature Compensation for Optical Fiber Graphene Micro-Pressure Sensor Using Genetic Wavelet Neural Networks. *IEEE Sensors Journal*, *21*(21), 24195–24201.

[26] Xie, J., Li, Z., & Zou, X. (2023). Dynamic Temperature Compensation of Pressure Sensors in Migratory Bird Biologging Applications. *Electronics*, *12*(20), 4373. https://doi.org/10.3390/electronics12204373

[27] Zhang, B., Tan, R., & Lin, C.-J. (2020). Forecasting of e-commerce transaction volume using a hybrid of extreme learning machine and improved moth-flame optimization algorithm. *Applied Intelligence*, *51*(2), 952–965. https://doi.org/10.1007/s10489-020-01840-y

[28] Lou, J., Jiang, Y., Shen, Q., Wang, R., & Li, Z. (2023). Probabilistic Regularized Extreme Learning for Robust Modeling of Traffic Flow Forecasting. *IEEE Transactions on Neural Networks and Learning Systems*, *34*(4), 1732–1741. https://doi.org/10.1109/tnnls.2020.3027822

[29] Li, J., Hong, Z., Zhang, C., Wu, J., & Yu, C. (2024). A novel hybrid model for crude oil price forecasting based on MEEMD and Mix-KELM. *Expert Systems with Applications*, *246*, 123104. https://doi.org/10.1016/j.eswa.2023.123104

[30] Bisoi, R., Dash, P.K., & Das, P.P. (2018). Short-term electricity price forecasting and classification in smart grids using optimized multikernel extreme learning machine. *Neural Computing and Applications*, *32*(5), 1457–1480. https://doi.org/10.1007/s00521-018-3652-5

[31] Sun, S., Wang, S., Wei, Y., & Zhang, G. (2020). A Clustering-Based Nonlinear Ensemble Approach for Exchange Rates Forecasting. *IEEE Transactions on Systems, Man, and Cybernetics: Systems*, *50*(6), 2284–2292. https://doi.org/10.1109/tsmc.2018.2799869

[32] Zou, M., Xu, Y., Jin, J., Chu, M., & Huang, W. (2023). Accurate Nonlinearity and Temperature Compensation Method for Piezoresistive Pressure Sensors Based on Data Generation. *Sensors*, *23*(13), 6167. https://doi.org/10.3390/s23136167

[33] Li, J., Hu, G., Zhou, Y., Zou, C., Peng, W., & Alam SM, J. (2017). Study on Temperature and Synthetic Compensation of Piezo-Resistive Differential Pressure Sensors by Coupled Simulated Annealing and Simplex Optimized Kernel Extreme Learning Machine. *Sensors*, *17*(4), 894. https://doi.org/10.3390/s17040894

[34] Liu, Y., & Wang, J. (2022). Transfer learning based multi-layer extreme learning machine for probabilistic wind power forecasting. *Applied Energy*, *312*, 118729. https://doi.org/10.1016/j.apenergy.2022.118729

[35] Qin, Q., Huang, Z., Zhou, Z., Chen, Y., & Zhao, W. (2022). Hodrick–Prescott filter-based hybrid ARIMA–SLFNs model with residual decomposition scheme for carbon price forecasting. *Applied Soft Computing*, *119*, 108560. https://doi.org/10.1016/j.asoc.2022.108560

[36] Lu, H., Ma, X., Huang, K., & Azimi, M. (2020). Carbon trading volume and price forecasting in China using multiple machine learning models. *Journal of Cleaner Production*, *249*, 119386. https://doi.org/10.1016/j.jclepro.2019.119386

[37] Sulaiman, S. M., Jeyanthy, P.A., Devaraj, D., & Shihabudheen, K.V. (2022). A novel hybrid short-term electricity forecasting technique for residential loads using Empirical Mode Decomposition and Extreme Learning Machines. *Computers & Electrical Engineering*, *98*, 107663. https://doi.org/10.1016/j.compeleceng.2021.107663

[38] Luo, J., & Liu, Z. (2019). Novel grey wolf optimization based on modified differential evolution for numerical function optimization. *Applied Intelligence*, *50*(2), 468–486. https://doi.org/10.1007/s10489-019-01521-5

[39] Mohanty, F., Rup, S., Dash, B., Majhi, B., & Swamy, M.N.S. (2018). A computer-aided diagnosis system using Tchebichef features and improved grey wolf optimized extreme learning machine. *Applied Intelligence*, *49*(3), 983–1001. https://doi.org/10.1007/s10489-018-1294-z

[40] Tong, S., Guo, M., Tian, Y., Le, J., Zhang, D., & Zhang, H. (2024). Multi-objective optimization design of scramjet nozzle based on grey wolf optimization algorithm and kernel extreme learning machine surrogate model. *Physics of Fluids*, *36*(2). https://doi.org/10.1063/5.0188627

[41] Roushangar, K., Shahnazi, S., & Sadaghiani, A.A. (2022). An efficient hybrid grey wolf optimization-based KELM approach for prediction of the discharge coefficient of submerged radial gates. *Soft Computing*, *27*(7), 3623–3640. https://doi.org/10.1007/s00500-022-07614-7

[42] Zhao, X., Chen, Y., Wei, G., Pang, L., & Xu, C. (2023). A comprehensive compensation method for piezoresistive pressure sensor based on surface fitting and improved grey wolf algorithm. *Measurement*, *207*, 112387. https://doi.org/10.1016/j.measurement.2022.112387

[43] Wen, X., Jaxa-Rozen, M., & Trutnevyte, E. (2022). Accuracy indicators for evaluating retrospective performance of energy system models. *Applied Energy*, *325*, 119906. https://doi.org/10.1016/j.apenergy.2022.119906

[44] Zhou, J., Lin, H., Jin, H., Li, S., Yan, Z., & Huang, S. (2022). Cooperative prediction method of gas emission from mining face based on feature selection and machine learning. *International Journal of Coal Science & Technology*, *9*(1). https://doi.org/10.1007/s40789-022-00519-8

Huan Wang (Graduate Member, IEEE) received the B.Sc. degree in Mechatronics Engineering from Nanjing Engineering College, China, in 2020. He received his M.Sc. degree in Aeronautical and Astronautical Science and Technology from the College of Aeronautics and Astronautics, Sun Yat-sen University in 2023. He is currently pursuing a Ph.D. degree from the School of Advanced Manufacturing, Sun Yat-sen University. His current research interests include the design of calibration system for multi-channel pressure scanners and the study of high precision temperature compensation algorithms.

Ting Wu received B.Eng. degree from the China University of Mining and Technology (CUMT), China in 2023. Since then, he has been pursuing a M.Eng. degree from Sun Yat-sen University (SYSU). His main research interests include sensor algorithms and control theory.

Pan Liu received his B.Sc. degree in Mechanical Engineering from the School of Mechanical Engineering and Automation at Northeastern University in Shenyang, Liaoning Province in 2017. He is currently pursuing a master's degree in Energy and Power at the School of Aeronautics and Astronautics at Sun Yat-sen University in Shenzhen, China. His research interests are temperature compensation and fault diagnosis of multi-channel pressure scanners.

Yijun Zou received the B.Sc. degree in detection guidance and control from the School of Astronautics, Northwestern Polytechnical University, Xi'an, China, in 2019. She is currently pursuing the M.Sc. degree in aerospace science and technology from Sun Yat-sen University, Shenzhen, China. Her current research interests in fault diagnosis of pressure sensor.

Qinghua Zeng received the Ph.D. degree in aerospace science and engineering from the National University of Defense Technology, Changsha, China, in 2003. He is currently a Professor with Sun Yat-sen University, Shenzhen, China. His research interests include aircraft control system design and simulation, and design of pressure measurement systems for solid rocket engines.